Systems & Control Transactions

Research Article - Peer Reviewed Conference Proceeding
ESCAPE 35 - European Symposium on Computer Aided Process Engineering
Ghent, Belgium. 6-9 July 2025
Jan F.M. Van Impe, Grégoire Léonard, Satyajeet S. Bhonsale, Monika E. Polańska, Filip Logist (Eds.)

PSE PRESS

Temporal Decomposition Scheme for Designing Large-Scale CO_2 Supply Chains Using a Neural Network-Based Model for Forecasting CO_2 Emissions

José A. Álvarez-Menchero*, Rubén Ruiz-Femenia, Raquel Salcedo-Diaz, Isabela Fons Moreno-Palancas, and José A. Caballero

University of Alicante, Department of Chemical Engineering, Alicante, Spain
* Corresponding Author: joseantonio.alvarez@ua.es .

ABSTRACT

The battle against climate change and the search for innovative solutions to mitigate its effects have become the focus of the researchers' attention. One potential approach to reduce the impacts of the global warming could be the design of a Carbon Capture and Storage Supply Chain (CCS SC). However, the high complexity of the model requires exploring alternative ways to optimise it. In this work, a CCS multi-period supply chain for Europe is designed. Data on CO_2 emissions have been sourced from the EDGAR database, which includes information spanning the last 50 years. Since this problem involves optimising the cost and operation decisions over a 10-year time horizon, it would be advisable to forecast carbon dioxide emissions to enhance the reliability of the data used. For this purpose, a neural network-based model is implemented for forecasting N-Beats. Furthermore, a temporal decomposition scheme is used to address the intractability issues of the model. The selected method is Lagrangean decomposition, which has been employed in other high complexity works, demonstrating strong performance and significant computational savings.

Keywords: Mathematical Programming, Generalized Disjunctive Programming, Supply chain, Mixed Integer Linear Programming, Lagrangean Decomposition, Time Series Forecasting, Deep learning.

1. INTRODUCTION

Over the last decades, climate change has become one of the main challenges that society must address. Consequently, many recent breakthroughs have focused on this issue. This is the case with CO_2 capture and storage supply chains, which have emerged as one of the most promising possible options to decarbonize the industrial sector. D'Amore, for example, proposes a European Carbon Capture and Storage Supply Chain (CCS SC) [1,2]. To achieve this, a Mixed Integer Linear Program (MILP) is implemented. As a result, the problem becomes computationally intractable for CO_2 reduction targets exceeding 70% due to its high complexity. A possible solution to overcome this difficulty might be the use of decomposition methods, such as the Lagrangean Decomposition [3]. Similarly, Jackson and Grossmann propose a temporal decomposition scheme based on this Lagrangean approach to solve a multiperiod nonlinear programming optimization model, obtaining satisfactory results [4]. Additionally, designing a supply chain over a time horizon involves inherent uncertainties, such as future CO_2 emissions. Therefore, it is crucial to explore methods to enhance data reliability.

Altogether, this paper implements a temporal decomposition technique based on Lagrangean Decomposition to design a CCS SC in the Iberian Peninsula. The model is optimized over a 10-year time horizon. As a result, the suitability of applying this resolution method to solve such complex problems is analyzed. Furthermore, a neural network-based model (N-BEATS) is implemented to forecast CO_2 emissions over the same 10-year time horizon [5].

2. PROBLEM STATEMENT

As mentioned earlier, this paper proposes a temporal decomposition technique based on Lagrangean decomposition to optimize a CCS SC within the Spanish and Portuguese territory over a 10-year time horizon.

The model is formulated as a grid-based, spatially explicit Mixed Integer Linear Program (MILP). Consequently, the territory is divided into smaller regions *g*. The CO_2 emissions for each region are sourced from the Emissions Database for Global Atmospheric Research (EDGAR) [6], which is a global database of anthropogenic emissions of greenhouse gases and air pollution on Earth. Additionally, potential CO_2 storage sites are obtained from the CO_2Stop Project database [7], which provides information on the locations and capacities of underground geological formations in Europe that could be suitable to store CO_2.

It is now necessary to define how the CO_2 is captured and transported. On the one hand, three different possible technologies *k* are considered regarding the CO_2 capture: post-combustion, pre-combustion and oxy-fuel combustion. On the other hand, they can be transported by onshore or offshore pipelines *L* depending on the region's location.

3. NOMENCLATURE

Sets

g	regions
k	capture technology {$post^{comb}$, pre^{comb}, oxy^{fuel}}
l	pipelines {onshore, offshore}
t	time period {1,2,…,10}
$CR_{g,g'}$	It is possible to connect g to g' by a pipeline

Parameters

α	CO_2 reduction target
$E_{g,t}$	Region g CO_2 emissions at time period t [10^7 tons]
S_g	Storage capacity in region g [10^9 tons]
UC_k	Capture technology k unitary cost [€/ton]
$FC_{g,g'}$	Pipeline between g and g' construction cost [€]
$OC_{g,g'}$	Pipeline between g and g' operational cost [€/year]
$D_{g,g'}$	Distance between g and g' [km]
C^{IR}	Intra-regional transport cost [€/(ton·km)]
$SIZE_g$	Region g size [km]
η_k	Capture technology k efficiency
$\gamma_{g,k}$	Technology k feasibility in region g according to fuels contribution to emission
Q^{MAX}	Transport capacity of the pipelines [10^7 tons/year]
C^{MAX}	Upper limit for the construction rate of pipelines [km/year]
CAP^{INJ}	Maximum injection well capacity [tons/year]
$depth_g$	Injection depth in region [km]
CCR	Capital cost rate for injection well
OM	Mainteneance rate for injection well

Continuous Variables

$p_{k,g,t}$	Processed CO_2 through technology k in region g at time period t [10^7 tons]
$c_{k,g,t}$	Captured CO_2 through technology k in region g at time period t [10^7 tons]
$q_{g,g',t}$	CO_2 transported from g to g' at time period t [10^7 tons]
$s_{g,t}$	CO_2 sequestred in region g at time period t [10^9 tons]

Binary Variables

$y_{g,g',t}$	Takes a value of 1 if a pipeline from g to g' is built
$\widehat{y_{g,g',t}}$	Duplicate of binary variable $y_{g,g',t}$

Integer Variables

$n_{g,t}^{wells}$	Number of injections well constructed in region g at time period t

In this model It is possible to identify three different problems:

- Capture Problem.
- Transport Problem.
- Sequestration Problem.

The capture problem is modeled using Eqs. (1-4). First, Eq. (1) defines that the total processed CO_2 in region g at time t cannot exceed its emissions $E_{g,t}$. Next, Eq. (2) sets the maximum CO_2 that can be processed by each technology k. Then, Eq. (3) specifies the minimum total CO_2 that must be processed across all regions g over the 10-year time horizon. Finally, Eq. (4) establishes the relationship between $c_{k,g,t}$ and $p_{k,g,t}$.

$$\sum_k p_{k,g,t} \leq E_{g,t}, \quad \forall g, \forall t \tag{1}$$

$$p_{k,g,t} \leq \gamma_{g,k} E_{g,t}, \quad \forall k, \forall g, \forall t \tag{2}$$

$$\sum_{k,g,t} \eta_k \, p_{k,g,t} \geq \alpha \sum_{g,t} E_{g,t} \tag{3}$$

$$c_{k,g,t} = \eta_k p_{k,g,t}, \quad \forall k, \forall g, \forall t \tag{4}$$

Regarding the transport problem, the mass balance is established in Eq. (5).

$$\sum_c c_{c,g,t} + \sum_{g' \in SR_{g,g'}} q_{g',g,t} = 100 s_{c,g,t} + \sum_{g' \in SR_{g,g'}} q_{g,g',t} \quad \forall g, \forall t \tag{5}$$

Additionally, as CO_2 transport from region g to region g' at time t depends on if the pipelines that connects both regions is built at that time, the Boolean variable $Y_{g,g',t}$ is defined. This Boolean variable is true if the pipeline to transport CO_2 from region g to region g' is built at time t.

The disjunctive model is formulated as follows:

$$\underset{(g,g' \in CR_{g,g'})}{\underline{\vee}} \begin{bmatrix} Y_{g,g',t} \\ q_{g,g',t} \leq Q^{MAX} \end{bmatrix}, \ t \in T \quad (6)$$

It is now necessary to establish that if a pipeline between a region g and a region g' is built at time t-1, then the pipeline will remain there at time t. The logical relationship which defines it is shown in Eq. (7).

$$Y_{g,g',t-1} \Rightarrow Y_{g,g',t}, \ \forall g \in CR_{g,g'}, \forall g' \in CR_{g,g'}, \forall t \quad (7)$$

Eqs. (6) and (7) reformulated in terms of binary variables are shown below in Eqs. (8) and (9).

$$q_{g,g',t} \leq Q^{MAX} y_{g,g',t}, \ \forall g, g' \in CR_{g,g'}, \forall t \quad (8)$$

$$y_{g,g',t} - y_{g,g',t-1} \geq 0, \ \forall g, g' \in CR_{g,g'}, \forall t \quad (9)$$

Furthermore, Eqs.(10) and (11) establish an upper limit to the total length of pipelines built throughout a year.

$$\sum_{g,g'} D_{g,g'} \left(y_{g,g',t} - y_{g,g',t-1} \right) \leq C^{\text{MAX}}, \quad \forall t > 1 \quad (10)$$

$$\sum_{g,g'} D_{g,g'} y_{g,g',t} \leq C^{MAX}, \quad t = 1 \quad (11)$$

Next, the sequestration problem is defined below:

$$\sum_t s_{g,t} = S_g, \quad \forall g \quad (12)$$

$$n_{g,t}^{wells} = \frac{s_{g,t}}{CAP^{INJ}}, \quad \forall g, \forall t \quad (13)$$

Eq. (12) sets the maximum CO_2 which can be store at each region as its storage capacity, and Eq. (13) defines the number of wells built at region g at time t.

Lastly, the objective function shown in Eq. 14 minimizes the total cost of the supply chain given by the cost of capturing the CO_2 plus the pipeline's construction and operational cost, the shipping cost and the storage cost.

$$\begin{aligned} min\ \Phi = {} & 10^{-1} \textstyle\sum_{k,g,t} UC_k\, \eta_k p_{k,g,t} + \\ & 10^{-8} \textstyle\sum_{g,g' \in SR_{g,g'}} FC_{g,g'}\, y_{g,g',T} + \\ & 10^{-8} \textstyle\sum_{g,g',t \in SR_{g,g'}} \text{OC}_{g,g'}\, y_{g,g',t} + \\ & 10^{-1} \textstyle\sum_{g,g',t \in SR_{g,g'}} \text{D}_{g,g'}\, \text{q}_{g,g',t} + \\ & 10^{-1} C^{IR} \textstyle\sum_{\text{k,g,t}} \text{SIZE}_g\, \gamma_k p_{k,g,t} + \\ & 10^{-8} \textstyle\sum_{g,t} (CCR + OM)\left(m_1 depth_g + m2\right) n_{g,t}^{wells} \end{aligned} \quad (14)$$

Notice that the model has been scaled in order to improve the numerical stability and efficiency of the solver.

4. SOLUTION STRATEGY

The Mixed Integer Linear Programming (MILP) described by Eqs. (1)-(14) can easily become an intractable problem as the number of regions g, the reduction target, or the time horizon increase. Therefore, given the model's structure, a decomposition method could be suitable to overcome these issues. The decomposition algorithm, outlined in Figure 1, follows the approach by Jackson and Grossmann [4].

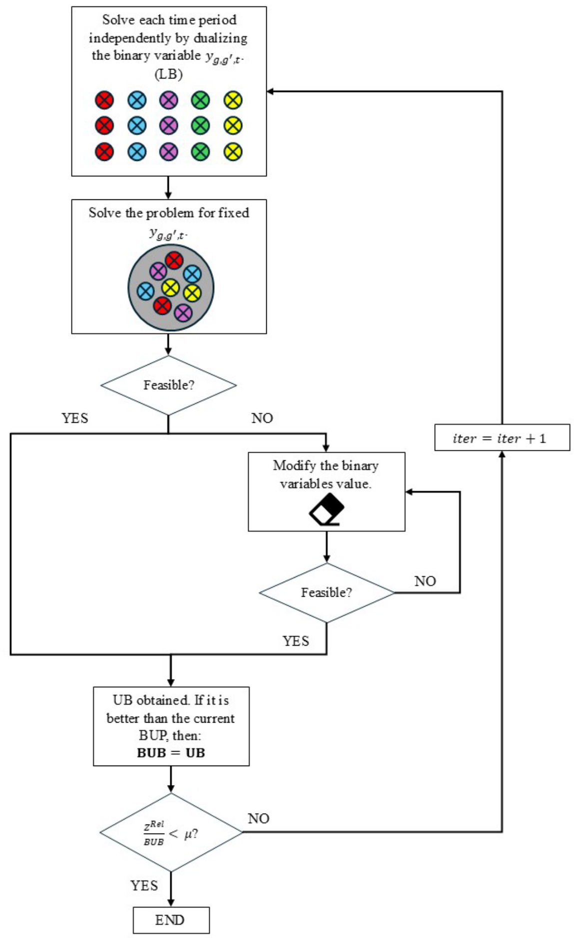

Figure 1. Decomposition algorithm steps.

We adopt a temporal decomposition scheme. To implement it, we first identify the constraints which couple the time periods. In this case, these constraints are Eqs. (9) and (10). Thus, the binary variables $y_{g,g',t}$ must be duplicated, as formulated in Eq. (15).

$$y_{g,g',t} = \widehat{y_{g,g',t}}, \quad \forall g \in CR_{g,g'}, \forall g' \in CR_{g,g'}, \forall t \quad (15)$$

Now, Eqs. (16) and (17) are obtained after rewriting the affected equations.

$$y_{g,g',t} - \widehat{y_{g,g',t-1}} \geq 0, \quad \forall g, \forall g', \forall t > 1 \quad (16)$$

$$\sum_{g,g'} \left[D_{g,g'} \left(y_{g,g',t} - \widehat{y_{g,g',t-1}} \right) \right] \leq C^{\text{MAX}} \quad (17)$$

Eq. (15), which is called interconnection constraint, is dualized so that the Lagrangean Decomposition is applied. After dualizing, Eq. (15) transforms into Eq. (18).

$$min\ \Phi_{LR} = \Phi + \sum_{g,g',t\in SR} \lambda_{g,g',t}\left(y_{g,g',t} - \widehat{y_{g,g',t}}\right) \quad (18)$$

As indicated in Figure 1, a lower bound is obtained once each subproblem is optimized. Then, the binary variables are fixed to the values given by the decomposed model and the original problem, comprising Eqs. (1)-(14) is solved. If the problem is infeasible, which is more likely due to the high number of variables, a strategy must be designed to modify the binary variables. The following algorithm is proposed to guarantee that a solution is achieved:

$If \quad \sum_t y^k_{g,g',t} \geq 2,$

Being Y the first time period t with $y^k_{g,g',t} = 1$, for all t $> Y$:

$$y^k_{g,g',t} = 1, \quad \forall t > Y$$

Else

$$y^k_{g,g',t} = 0, \quad \forall t$$

Figure 2. Binary variables modification algorithm

Lastly, Eqs. (19) and (20) update the Lagrange multipliers $\lambda_{g,g',t}$, ensuring convergence across iterations.

$$step^k = 0.5\frac{LB_k - UB}{\sum_{g,g',t}\left(y^k_{g,g',t} - \widehat{y^k_{g,g',t}}\right)^2} \quad (19)$$

$$y^{k+1}_{g,g',t} = y^k_{g,g',t} - step^k\left(y^k_{g,g',t} - \widehat{y^k_{g,g',t}}\right) \quad (20)$$

5. CO_2 EMISSIONS FORECAST

As mentioned earlier, N-BEATS is the neural network-based model selected for forecasting CO_2 emissions. This section explains the methodology implemented to select the most suitable model.

5.1 Exploratory Data Analysis

Given a dataset containing multiple series, Exploratory Data Analysis is conducted to identify potential correlation between the series and exploit this knowledge to enhance the training process.

In this regard, cross-correlation is a widespread tool to assess the degree of correlation between two time series. We compare series pairwise by computing its Pearson correlation coefficient and visualize the results with the aid of heatmaps. The Pearson correlation coefficient is shown in Eq. (21).

$$\rho_{x,y} = \frac{cov(X,Y)}{\sigma_x \sigma_y} \quad (21)$$

Where X and Y represent two different time series.

As this metric might be affected by the autocorrelation among preceding lags, this within-series dependence must be first removed. This is achieved by recursively differencing each series until the ADF test proofs its stationarity.

5.2 Data preprocessing

Before training forecasting models, historical data was normalized for convenience using min-max normalization

$$x_{scaled} = \frac{x - x_{min}}{x_{max} - x_{min}} \quad (22)$$

Then, data was also split into train (80%), validation (10%) and test (10%) sets.

5.2 Model Selection

The model architectures studied are shown in Figure 3.

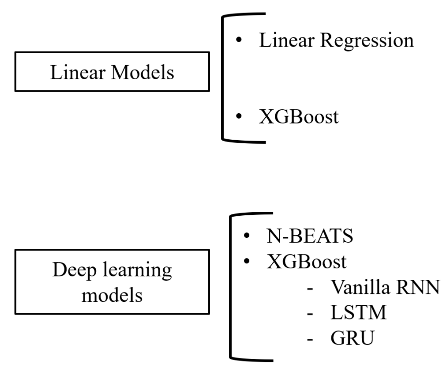

Figure 3. Model architectures studied.

Their performance was benchmarked against a baseline model, namely, the moving average of the last two preceding values.

For each model type, the best hyperparameter configuration (BHC) was search inside a predefined search space. While a grid search approach was preferred for regression models, the tuning process of deep learning models was carried out using the open-source library Optuna [5]. The BHC was found by training different models varying the hyperparameter values, evaluating its mean absolute percentage error (MAPE) on the validation set and using the minimum MAPE as selection criteria.

For neural network-based models, the learning rate of the model with the BHC was further refined given the impact of this hyperparameter on model performance. This was achieved by running the training process again, this time increasing the learning rate after each batch is processed. The evolution of the loss function is logged, and loss vs. learning rate plots are used as guidance for choosing a good value of this hyperparameter.

Next, the model with the BHC found so far was retrained on the whole training set (concatenation of test and validation sets), and its performance was evaluated on the test set.

Finally, the model reporting the lowest MAPE in the test set will be the one selected to generate future forecasts.

5.3 Results

The heatmap in Figure 4 represents the cross-correlation between the CO_2 emissions in the regions considered for this case study. It evidences strong correlations among the CO_2 emissions in regions, as is the case of regions 26 and 14.

The results of the model selection process are shown in Table 1. For comparison purposes, all models were trained for 200 epochs, using a batch size of 32, and the forecasts are obtained one year at a time.

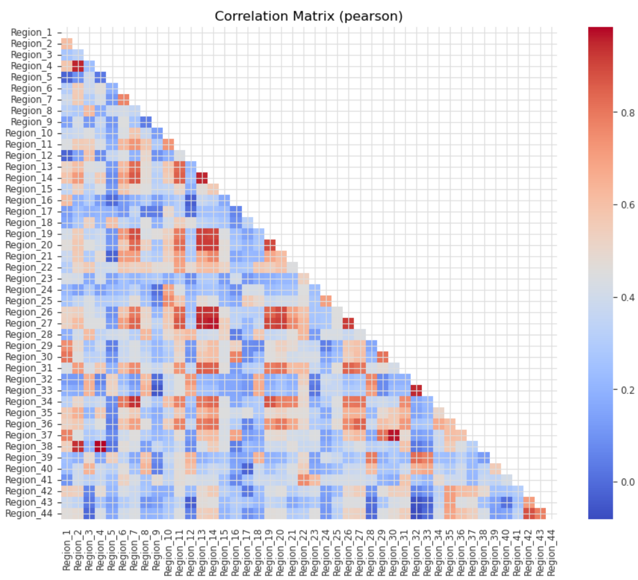

Figure 4. Heatmap of Pearson correlation coefficient.

Table 1: Results of tuning process and performance on the test set.

	$MAPE_{test}$	BHC
Moving average	14.31%	window size = 2
Linear Regression	14.63%	lags = 4
XGB	14.96%	lags = 2
N-BEATS	14.16%	input_chunk 3
		num_blocks = 2
		num_layers = 4
		num_stacks = 2
		layer_width = 256
		batch_size = 32
		learning_rate = 10^{-4}
RNNs	15.13%	Model type: LSTM
		num_layers = 4
		input_chunk = 4
		batch_size = 32
		learning_rate=$2\cdot10^{-3}$
		optimizer = ADAM

In light of the results shown in Table 1, N-BEATS model was selected to forecast CO_2 emissions for a 10-year time horizon.

6. RESULTS AND DISCUSSION

The model was implemented in GAMS 46.5.0 and solved using Gurobi 11.0.1 solver. All code was executed on an Intel® Core™ i7-4790 CPU (3.60 GHz) with 8.00 GB RAM. The results are presented in Table 2.

Table 2. Optimization results.

	No. of iterations	Solution time (s)	Solution obtained	Gap (%)
Full-Space	-	8’26	1180.74	-
Lag. Dec.	47	13’ 44”	1257.13	6.47

As observed, the Lagrangean decomposition algorithm provides a good solution to this problem. However, it requires a significant amount of computational time to close the gap between the lower and upper bounds. Since this method is intended to be applied to problems of higher complexity, the proposed algorithm shown in Figures 1 and 2 needs to be improved. The supply chain obtained at the end of the 10-year time horizon is displayed in Figure 5.

7. CONCLUSION

The decomposition algorithm has demonstrated its effectiveness. However, further research is needed to improve the algorithm shown in Figure 2 and enhance the proposed resolution method, as it requires many iterations to close the gap.

Regarding the time series forecast, although N-BEATS proved to be the best model (Table 1), it performed only slightly better than a simple linear regression when applied to this case. This is due to the small size of the dataset used for forecasting. If a larger dataset had been used, the difference between the two methods would have been considerably greater.

ACKNOWLEDGEMENTS

The authors gratefully acknowledge financial support of the Spanish “Ministerio de Ciencia, Innovación y Universidades” under project PID2021-124139NB-C21. They would also like to thank “Generalitat Valenciana: Conselleria d’Educació, Cultura, Universitats i Ocupació” and the European Social Fund Plus (ESF+) for the PhD grant (CIACIF/2023/117).

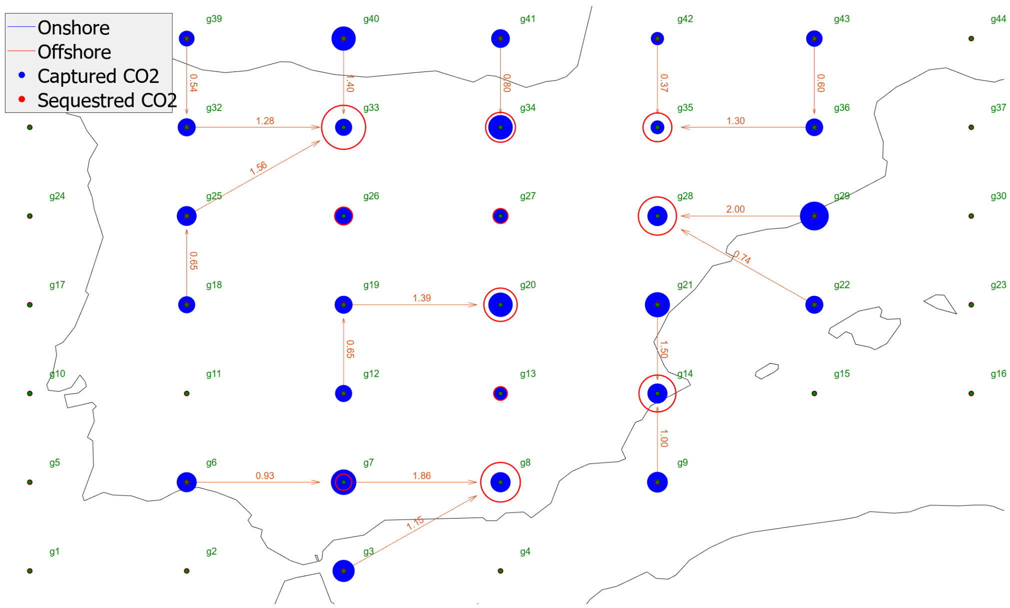

Figure 5: Carbon Capture and Storage Supply Chain obtained.

REFERENCES

1. D'Amore, F, Bezzo, F. Economic optimisation of European supply chains for CO_2 capture, transport and sequestration. *Int J Greenh Gas Control* 65:99-116 (2017) https://doi.org/10.1016/j.ijggc.2017.08.015
2. D'Amore, F, Romano, MC, Bezzo, F. Economic optimisation of European supply chains for CO_2 capture, transport and sequestration. *J Clean Prod* 290 (2021) https://doi.org/10.1016/j.jclepro.2020.125202
3. Guignard, M, S. Kim. Lagrangean Decomposition: A model yielding Stronger Lagrangean Bounds. *Math Program* 39:215-228 (1987) https://doi.org/10.1051/ro/1987210403071
4. Jackson JR, Grossmann IE. Temporal decomposition scheme for nonlinear multisite production planning and distribution models. Ind Eng Chem Res 42:3046–3054 (2003) http://dx.doi.org/10.1021/ie030070p
5. Akiba, T, Sano, S, Yanase, T, Ohta, T, Koyama, M. Optuna: A Next-generation Hyperparameter Optimization Framework. *Proc 25th ACM SIGKDD Int Conf Knowl Discovery Data Mining* 2623-2631 (2019) https://doi.org/10.48550/arXiv.1907.10902
6. Joint Research Centre. Emission Database for Global Atmospheric Research (EDGAR). https://edgar.jrc.ec.europa.eu/index.php
7. Joint Research Centre. CO_2 Storage Potential in Europe (2020) https://setis.ec.europa.eu/european-co2-storage-database_en